

Excitation of remarkably nondispersive surface plasmons on a nondiffracting, dual-pitch metal grating

Alastair P. Hibbins^{a)} and J. Roy Sambles

Thin Film Photonics Group, School of Physics, University of Exeter, Exeter, EX4 4QL United Kingdom

Chris R. Lawrence

QinetiQ (Structures and Materials Centre), Farnborough, GU14 0LX United Kingdom

(Received 19 November 2001; accepted for publication 4 February 2002)

A nondiffracting metallic lamellar grating formed from three equally spaced grooves per repeat period, with one being slightly shallower than the other two is examined at microwave frequencies. When filled with a slightly lossy dielectric, this structure supports a remarkably nondispersive surface plasmon polariton mode, which exhibits strong selective absorption of incident power. Measured reflectivities show excellent agreement with the results predicted by a rigorous coupled wave theory. © 2002 American Institute of Physics. [DOI: 10.1063/1.1465518]

The propagation of a surface plasmon polariton (SPP) along the planar interface between a metal and a dielectric is well understood.¹ For an ideal metal, whose electron system behaves as a free-electron gas, the dispersion of the SPP mode at the interface can be described by the equation

$$k_{SPP}^2 = \left(\frac{\omega}{c}\right)^2 \left[\frac{\varepsilon_d(1 - \omega_p^2/\omega^2)}{\varepsilon_d + (1 - \omega_p^2/\omega^2)} \right],$$

where k_{SPP} is the wave vector of the SPP, ω is frequency (in radians per second), c represents the speed of light in a vacuum, ε_d is the permittivity of the dielectric (assumed to be frequency independent), and ω_p is the plasma frequency of the metal. Hence, in the long wavelength limit, $\omega \ll \omega_p$, the dispersion of the SPP will follow the light line. However, the presence of any periodicity at the boundary not only causes diffraction, but also perturbs the mode's dispersion, splitting it into a series of bands that shows similarity to the way that the electron states in a periodic potential split.

It is known from previous studies that very flat SPP bands may be formed on deep metal gratings where each band corresponds to a standing wave SPP mode localized in the grating grooves.² An alternative profile has recently been suggested by Tan *et al.*³ who theoretically model the electromagnetic response of a short pitch grating whose structure is based on a primary deep short-period component and a shallow long-period component. Their results reveal the possibility of coupling to an infinite set of flatbanded SPPs, but clearly the manufacture of such a grating profile is extremely difficult, especially on the scale studied in the earlier-mentioned work ($\lambda_g = 30$ nm). In the present study we scale up this profile for use at microwave frequencies by forming a lamellar version in an aluminum-alloy substrate (Fig. 1). Each grating period is formed from three equally spaced grooves of the same widths, but with one groove shallower than the other two. Hence, the sample has a fundamental grating wave vector of $k_g = 2\pi/7.2$ mm⁻¹ and its profile, $A(x)$, may be represented by the infinite Fourier Series,

$$A(x) = a_1 \sin(k_g x + \phi_1) + a_2 \sin(2k_g x + \phi_2) + \dots \\ + a_N \sin(Nk_g x + \phi_N) + \dots,$$

where a_N represents the Fourier amplitude of the N -1 harmonic and ϕ_N is its associated phase shift.⁴ Figure 2 illustrates the first 18 terms of this series representing the profile shown in Fig. 1 (black bars) compared with those representing a profile of the same pitch, but with all the grooves of depth 2.2 mm (white bars). It is clear that while the uniform depth profile is represented only by the $N=3,6,12,15,\dots$ terms, whose amplitudes decrease as N is increased, Fourier analysis of the dual-pitch grating yields a more complicated series. Interestingly, while the additional terms in the analysis of the dual-pitch grating are small compared to the dominant $N=3,6,12,15,\dots$ terms, they play a crucial part in the electromagnetic response of the structure. Consider initially just the first three terms of the Fourier series that represents the structure whose grooves are all the same depth. Since $a_1 = a_2 = 0$, the profile is simply a deep sinusoid, and with a pitch of $\lambda_g/3$, it does not support diffracted orders for $\lambda_0 \geq 5.4$ mm. For this profile, the a_3 term (which is associated with the $3k_g$ grating wave vector) will set up two counter-propagating SPP modes at the Brillouin zone boundary and a band gap is established. Therefore, at the point where the dispersion curve meets the Brillouin zone boundary, the group velocity and the gradient of the curve must be zero. Figure 3(a) illustrates a schematic representation of the dispersion of the SPP mode supported by this uniform groove

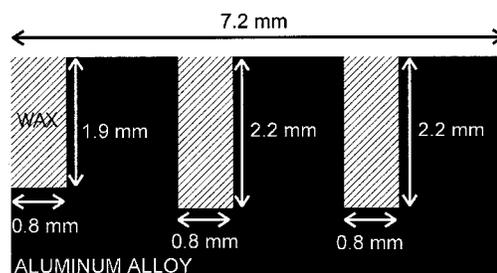


FIG. 1. Schematic diagram of one repeating unit of the profile studied in this work.

^{a)}Electronic mail: a.p.hibbins@exeter.ac.uk

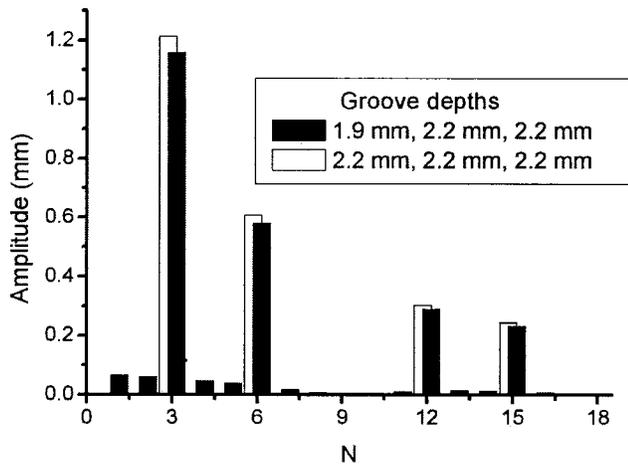


FIG. 2. The first 18 amplitudes of the Fourier series that represents the profile studied in this letter compared with the series for a profile with the same pitch, but uniform groove depths.

depth grating. Since the pitch of the grating is $\lambda_g/3$, the Brillouin zone boundary occurs at $k_x = 3k_g/2$ (marked ①), at which point a band gap may be observed although only the lower energy band is shown here. Notice that, since no part of this dispersion band appears inside the incident light lines, the mode is nonradiative being evanescently localized at the metal surface.

In order to couple radiation into the lowest order evanescent mode, it is necessary to convolve the original sinusoid with a shallow, longer pitch oscillation. For example, if a_1 takes a finite value, such that $a_1 \ll a_3$ (and $a_2 = 0$), there will be a long pitch component (λ_g) that will not significantly perturb the SPP dispersion curve but which will introduce important band-folding effects that cause an enormous change to the electromagnetic response of the metal structure. This is because the section of the dispersion curve of the high-momentum, nonradiative SPP mode is folded back into the area bordered by the light lines [Fig. 3(b)]. The

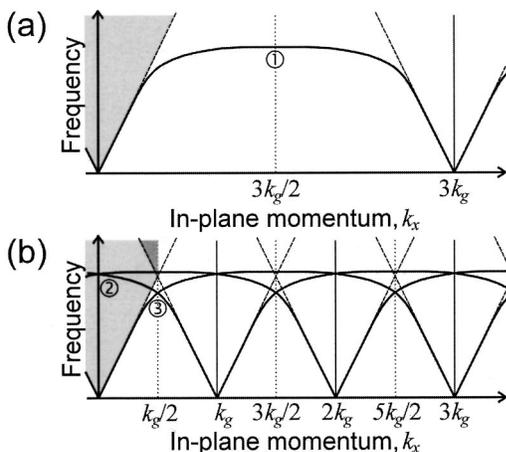


FIG. 3. (a) Schematic representation of the dispersion of the lowest-energy branch of the SPP supported by a grating similar to that illustrated in Fig. 1, but with all the grooves of the same depth. The shaded area bordered by the light line (dashed) represents the region of momentum space within which an incident photon may couple to a mode. (b) The effect of shallowing the depth of one in every three grooves. Note that for clarity, the band gaps that form at the points marked ② and ③ are not considered. The region shaded dark gray presents the momentum space within which the grating is no longer zero order.

result of this is that the originally nonradiative modes now become excitable by incident radiation leading to potentially strong resonant absorption. Note that a weakly coupled curved band, associated with a bandfolding about k_g is also to be expected.

Figure 3(b) is a very much-simplified illustration of the band structure of the modes supported by the dual-pitch system, and only takes into account the band gap that opens up at $k_x = 3k_g/2$. Further, smaller band gaps will also appear at other points in the band structure where two modes cross (marked ② and ③). It is also important to remember that the grating profile studied in this letter cannot accurately be described by a two-term Fourier series, but it is easy to see that the inclusion of the extra harmonic components will not greatly perturb the dispersion of the mode.

While Tan *et al.* consider the band structure in the vicinity of $\omega_p/\sqrt{2}$ (the surface-plasmon frequency of a planar surface, which for silver is $\sim 10^{15}$ Hz), the present experimental study has been undertaken in the microwave regime ($\sim 10^{10}$ Hz). It is important to note that at these frequencies, only perturbation of the lowest energy SPP band may be observed. In addition, since metals behave as near-perfect conductors, any modes excited on this structure will approximate to delta functions since there is no mechanism into which energy associated with the SPP can be lost. Therefore, in order to experimentally observe the excitation of the SPP mode over a sensible range of angles, the grating grooves are filled with petroleum wax, which is slightly absorbing at these frequencies ($\epsilon = 2.29 + 0.06i$).⁵

A parallel beam is incident upon the sample at a fixed polar angle⁵ (θ) and microwave-absorbing material is used where necessary to restrict the beam spot size to the region of the substrate in which the grating is machined. Incident radiation in the wavelength range $11.3 < \lambda_0 < 16.7$ mm is linearly p polarized (TM), with the grating grooves orientated so that they are normal to the plane of incidence (classical mount).

The experimental results are compared with the predictions from the GSOLVER program (Grating Solver Development Company, Texas), which is based on a full vector implementation of rigorous coupled wave theory. In order to obtain reliable data from this model, the number of orders retained in the calculation is increased systematically until convergent data are obtained. A Drude model is used to describe the dielectric function of the metal in the theoretical modeling.

Figure 4 shows a wavelength-dependent reflectivity plot, where the intensity of p -polarized radiation has been recorded with the beam incident at $\theta = 52.8^\circ$. Also shown is the response predicted for this structure by the GSOLVER software. This is in excellent agreement despite two issues associated with experiments of this kind which violate the assumptions made in the theoretical modeling—the finite size of the sample and some angle spread in the incident beam (approximately 1°).⁶ With the beam incident at $\theta = 52.8^\circ$, the grating will not support diffracted orders for wavelengths greater than the first-order Rayleigh anomaly, which is visible in Fig. 4 at $\lambda_0 \approx 13$ mm. (The Rayleigh anomaly corresponds to the point at which a diffracted order emerges from the grating surface at a grazing angle, resulting in a sudden

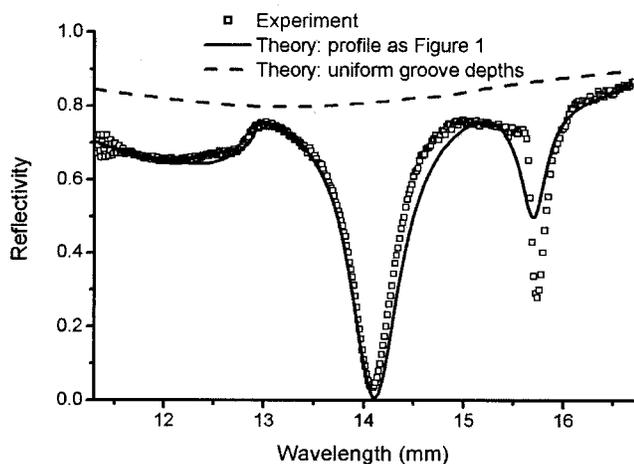


FIG. 4. Experimentally measured wavelength-dependent p -polarized reflectivity from the structure illustrated in Fig. 1 which is orientated in the classical mount with the microwave beam incident at 52.8° . The solid line represents the modeled response calculated using GSOLVER. Also shown is the modeled reflectivity from a similar grating profile but with all the grooves 2.2 mm deep (dashed line).

redistribution of the available energy.) In addition, the grating is orientated in the classical mount and, hence, no polarization conversion may occur.⁷ Therefore, any reduction in reflectivity must be accompanied by a matching increase in absorption. On resonance of the mode at $\lambda_0 = 14.1$ mm, our results indicate that more than 96% of the incident power is being absorbed by the structure. In contrast to this, the mode at $\lambda_0 = 15.7$ mm is much less well coupled. For comparison, the modeled reflectivity from a similar structure but with all the grooves 2.2 mm deep, again illuminated at $\theta = 52.8^\circ$, is also shown. As predicted by Fig. 3(a), no sharp modes are observed.

In order to identify and study the dispersion of each of these features, frequency-dependent reflectivity scans have been recorded at a further six different fixed polar angles of incidence. The frequencies (in gigahertz) of each of the observed resonances and Rayleigh anomalies are plotted in Fig. 5 against their associated value of in-plane momentum, $k_x = (2\pi f/c)\sin\theta$ (where frequency, $f = \omega/2\pi$), and are superimposed on top of a greyscale map representing the theoretically modeled response of the structure. Of course the most important feature of Fig. 5 is the flat resonance band that extends almost completely from normal to grazing incidence at approximately 21.3 GHz ($\lambda_0 \sim 14$ mm). Reflectivity levels on resonance of this mode are always less than 15% for $\theta < 70^\circ$ ($2k_x/k_g < 0.96$); beyond which the mode is perturbed by its approach to the Brillouin zone boundary and its proximity to the incident light line (at which the reflectivity must be unity).

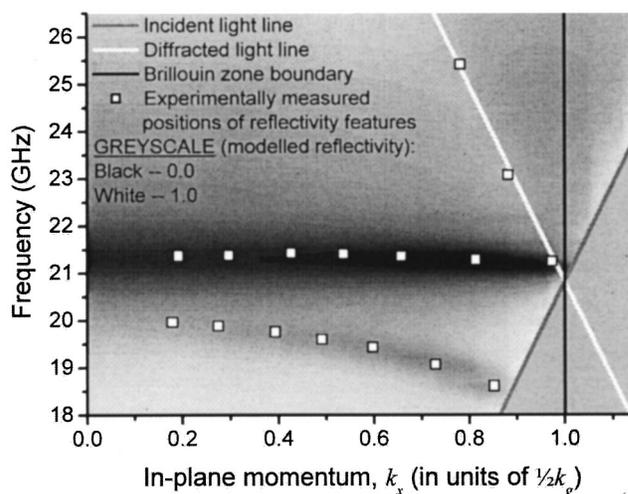


FIG. 5. Greyscale map of the modeled reflectivity illustrating the dispersion of the modes supported by the structure, on top of which are overlaid the positions of the reflectivity features obtained from the experiment.

In this work we have studied a dielectric filled, dual-pitch, aluminum-alloy grating at microwave frequencies. While the deep, short pitch component of the profile creates the flatbanded SPP mode outside the light line, it is the shallow long pitch component that provides the necessary extra in-plane momentum to allow incident photons to couple to this high-momentum region of the dispersion curve. The net result is a structure that, when correctly orientated with respect to the incident beam, demonstrates remarkable angle-independent excitation of the SPP mode and selective absorption of the incident power, powerfully illustrating the potential of “designer” surfaces of very short pitch. Our experimental observations, which have been recorded as a function of wavelength at seven different angles of incidence, show excellent agreement with the predictions from a rigorous coupled wave theory.

This work was carried out as part of Technology Group 09 of the MoD Corporate Research Program.

¹H. Raether, *Surface Plasmons* (Springer, Berlin, 1988).

²J. R. Andrewartha, J. R. Fox, and I. J. Wilson, *Opt. Acta* **26**, 197 (1979); E. Popov, L. Tsonev, and D. Maystre, *Appl. Opt.* **33**, 5214 (1994); F. J. Garcia-Vidal, J. Sanchez-Dehesa, A. Dechlette, E. Bustarret, T. Lopez-Rios, T. Fournier, and B. Pannetier, *J. Lightwave Technol.* **17**, 2191 (1999).

³W. C. Tan, J. R. Sambles, and T. W. Preist, *Phys. Rev. B* **61**, 13177 (2000).

⁴A. C. R. Pipino and G. C. Schatz, *J. Opt. Soc. Am. B* **11**, 2036 (1994).

⁵A. P. Hibbins, J. R. Sambles, and C. R. Lawrence, *Phys. Rev. E* **61**, 5900 (2000).

⁶A. P. Hibbins, J. R. Sambles, and C. R. Lawrence, *J. Appl. Phys.* **86**, 1791 (1999).

⁷S. J. Elston, G. P. Bryan-Brown, T. W. Preist, and J. R. Sambles, *Phys. Rev. B* **44**, 3483 (1991).